



# Study of thin film composites based on $\text{LiCoO}_2$ and $\text{C}_{60}$ using neutron depth profiling and atomic force microscopy

Giovanni Ceccio<sup>1</sup> · Jiri Vacik<sup>1</sup> · Vasyl Lavrentiev<sup>1</sup> · Ivo Tomandl<sup>1</sup> · Romana Miksova<sup>1</sup> · Kazumasa Takahashi<sup>2</sup>

Received: 4 July 2024 / Accepted: 31 August 2024  
© The Author(s) 2024

## Abstract

In this work, two thin hybrid composites based on organic-like fullerenes (bucky balls  $\text{C}_{60}$ ) and inorganic compounds of lithium cobalt oxide ( $\text{LiCoO}_2$ ) were prepared. The composites were synthesized by a combined method of ion sputtering and evaporation. The prepared samples were sandwiched between 2 gold electrodes and subjected to charging at an applied small voltage. After each charging process, the samples were analyzed using two appropriate methods—the surface morphology was monitored using AFM (Atomic Force Microscopy), and lithium depth concentration profiles were measured using NDP (Neutron Depth Profiling). The results of the measurements showed that both types of composite experienced significant changes both in the surface morphology and especially in the depth distribution of lithium. The test confirmed the expectation that the unusual hybrid combination of organic and inorganic phases is electrochemically active and exhibits characteristics of Li battery behavior.

**Keywords**  $\text{LiCoO}_2$  · Fullerene  $\text{C}_{60}$  · Thermal neutron depth profiling · Atomic force microscopy · Diffusion

## Introduction

Currently, a constant motive of research is the effort to create various devices for sustainable transformation, conversion and storage of energy, which would help to solve the growing problems of gradual consumption of non-renewable energy sources. Energy storage systems that are easily accessible to the end user play a vital role. These are primarily batteries of various types, parameters and sizes, which are of considerable interest due to the ever-growing needs for portable electronics, electric vehicles, smart grids, etc. [1]. Since the development of Li-ion batteries has reached the stage where the full (i.e., theoretical) capacity of the cathodes can be used [2], the next step is the development of a new high-performance electrolyte that would allow the use of all high-voltage battery possibilities and which would avoid destructive pitfalls such as is the formation of dendrites that quickly shorten the life of the battery. However, research

into new electrolytes is still in its infancy. For this purpose, some operational methods are used, which allow information about the movement of Li ions as charge carriers in real time. This is, for example, a non-destructive method of neutron depth profiling, which was successfully applied in the study of a new lithium conductive glass-ceramic electrolyte [3], and which is also used in this work. The next step in the development of Li ion batteries can be considered the preparation of complex hybrid composites as a form of ultra-thin battery systems, which would make it possible to combine non-traditional materials from opposite realms with unique (also electrochemical) properties. They would help to prepare thin batteries, e.g., with very high-rate capability and long cycle life. One of the possible hybrid forms can be electrodes based on fullerenes and a suitable inorganic material. The next step would be to select a solid hybrid electrolyte with high electrolyte diffusion ability and low internal resistance.

In this work, we made an attempt to combine 2 materials of such kind (showing the desired electrochemical activity), which (according to the information available to us) have not yet been tested as a closed battery system. In addition to fullerenes in this experiment we chose lithium cobalt oxide ( $\text{LiCoO}_2$ ), which is currently widely used mainly in rechargeable lithium-ion batteries as the cathode [4]. In this

✉ Giovanni Ceccio  
ceccio@ujf.cas.cz

<sup>1</sup> Neutron Physics Department, Nuclear Physics Institute of CAS, Řež 130, Husinec 250 68, Czech Republic

<sup>2</sup> Department of Electrical Engineering, Nagaoka University of Technology, Nagaoka, Japan

pilot test, we chose 2 types of composites—(i) on the one hand, the traditional structure of a composite assembled as a  $C_{60}/LiCoO_2$  multilayer consisting of a  $LiCoO_2$  buffer nanolayer and a  $C_{60}$  nanolayer, both sandwiched between thin gold current collectors, and then (ii) a composite created by an unconventional combination (co-deposition) of both phases, i.e.,  $LiCoO_2 + C_{60}$ . This composite was also sandwiched between 2 thin Au current collectors. For the preparation of both types of hybrid composites, methods using sputtering of the solid target material using ions and evaporation of the powder material by heating were used.

The aim of the study was to find out:

- (i) what quality and integrity of the composites can be achieved by the applied deposition methods (for this purpose two relevant analytical techniques AFM (Atomic Force Microscopy) and NDP (Neutron Depth Profiling) were used, and mainly.
- (ii) what are the responses of the composites to the applied voltages, i.e., how does the surface morphology change and what is the evolution of the depth concentration profiles of lithium.

## Experimental

The experiments were performed in the laboratories of the NPI infrastructure - ‘Center of Accelerators and Nuclear Analytical Methods’ (CANAM) [5]. Analyzes requiring a beam of thermal neutrons were carried out on the LVR-15 reactor operated by the Czech International Center of Research Reactors—CICRR [6] using the ‘Rez reactors’ (RC) infrastructure [7].

For the preparation of thin layers of composites based on  $LiCoO_2$  (99.9%, MTI Corp.) and bucky balls  $C_{60}$  (99.5%, Fisher Scientific), an unconventional method was applied consisting of a combination of ion sputtering (IBS) (of a 2-inch target  $LiCoO_2$ ), a method installed for the given study at the Low Energy Ion Facility (LEIF) system [5], and evaporation of fullerenes [8] using an effusion cell located in a sputtering chamber.  $Ar^+$  ions with an energy of 20 keV and a current of approx. 1 mA were chosen for IBS. The beam was focused in the ion-optical part of the system on an area of approx.  $1\text{ cm}^2$  at the target location. The distance of the target from the substrate was selected to be about 10 cm, the same distance was also maintained between the fullerene effusion cell and the substrate. The maximum area size of the substrate was chosen to be  $15 \times 15\text{ cm}^2$ , so that the deposited layer was still relatively homogeneous and it was possible to perform analyzes (see below) requiring a larger area of sample to achieve relatively high measurement statistics (i.e., a high detection rate in reactions with neutrons). The deposition rates and

thicknesses of the layers corresponding to  $LiCoO_2$  and  $C_{60}$  (or their combination) were continuously controlled by a thickness monitor (Inficon); during deposition, the head of the measuring probe was kept approximately in the same plane (i.e., at the same distance from the target and the effusion cell) as the deposited substrates—Si wafers ( $0.5\text{ mm}$ , size  $15 \times 15\text{ mm}^2$ ). Before the actual preparation of the composites, the deposition rates of building elements (Li, Co) were measured under selected angles of incidence of ions during sputtering. This made it possible to estimate in which stoichiometric ratio the building elements will be sputtered during the preparation of composites. It was shown (and later RBS analysis confirmed it) that, despite some differences, the desired  $LiCoO_2$  composite is recreated during codeposition of the building elements, with some excess of Li (due to the higher sputtering rate) agglomerating outside the main part of the composite.

Thin mixes and thin multilayers of sputtered material ( $LiCoO_2$ ) and evaporated fullerenes ( $C_{60}$ ) were designed and prepared for the experiment. In order to be able to compare the results of the analyzes for both types of composite, the samples were prepared in such a way that they contained approximately the same amount of the corresponding structural elements (e.g., the same amount of lithium for both types of composite). For the charging process, the composites were sandwiched between the thin gold current collectors (for comparison purposes, a part of the surface was left without Au coating for several samples). During the preparation of the composite assembly, part of the bottom collector (deposited directly on the Si substrate) was covered with a shield so that it could be used for electrical connections for charging processes. The thin hybrid assemblies were created for the experiment as follows (thicknesses shown for each component of the composite are only approximate):

- $Au(100\text{ nm})/LiCoO_2 + C_{60}(500\text{ nm})/Au(100\text{ nm})//Si_{\text{substrate}}$
- $Au(100\text{ nm})/LiCoO_2(300\text{ nm})/C_{60}(200\text{ nm})/Au(100\text{ nm})//Si_{\text{substrate}}$

Figure 1 schematically shows the design, how the composites with gold current collectors were prepared, and how their electrical connection was designed for charging using a potentiostat/galvanostat type PGSTAT 204. The electrical connection was realized using thin gold wires (thickness of  $0.1\text{ mm}$ ), connection to the Au collector was done using conductive Ag paste, connecting the wires to the BNC connector of the electrostat by soldering.

After the overall preparation (i.e., deposition of  $LiCoO_2$  by IBS and  $C_{60}$  by effusion cell, and after connecting the contacts), the composites were charged in a defined manner (under  $\sim 1\text{ mbar}$  vacuum) for 24 h at voltages of 50 mV,

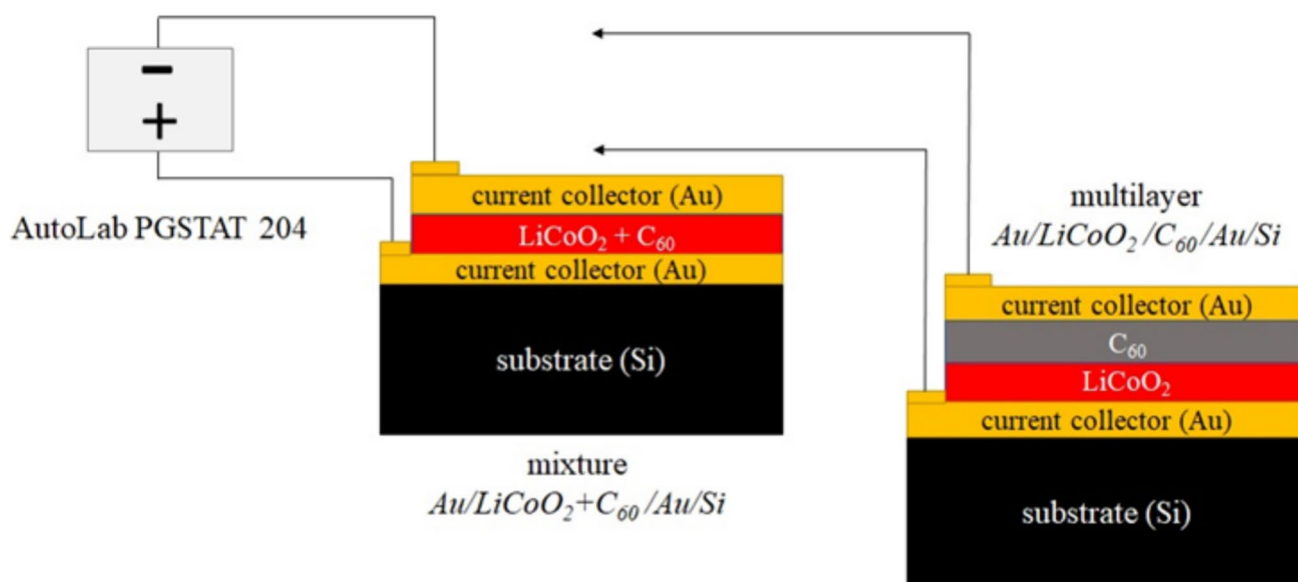


**Fig. 1** Schematic sketch of a mix ( $\text{LiCoO}_2 + \text{C}_{60}$ ) and a multilayer ( $\text{C}_{60}/\text{LiCoO}_2$ ) deposited as thin composites between Au charge collectors on a Si wafer, and their connection for the charging process using an AutoLab PGSTAT 204 potentiostat/galvanostat

100 mV, 500 mV, and 1000 mV (with mixture  $\text{LiCoO}_2 + \text{C}_{60}$  charging at 1 V was not possible, several attempts led to the destruction of its microstructure).

The prepared samples were subsequently analyzed by the AFM (Atomic Force Microscopy) method, where their surface morphology and its dynamic changes after the application of the applied voltages were monitored. For this purpose, the NTEGRA Aura microscope (NT-MDT Ltd.) was used with the tapping mode (using the NSG10 AFM cantilevers) performed in ambient conditions. It enabled a detailed analysis of the surface morphology with a spatial resolution  $< 1$  nm.

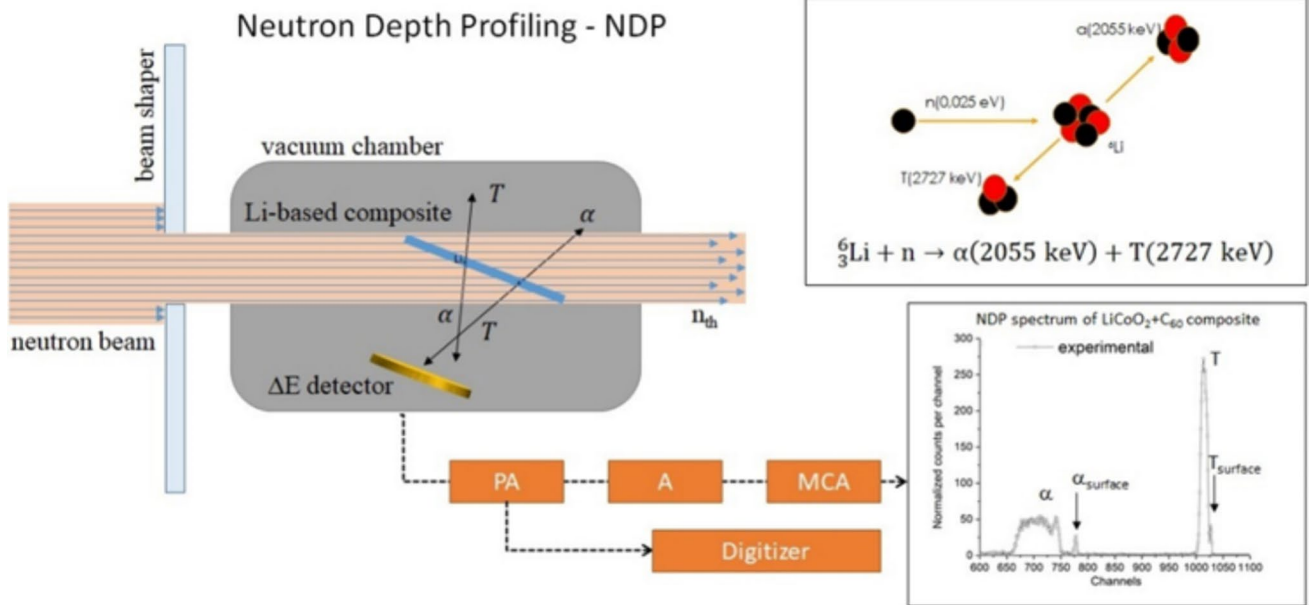
The large-scale samples were further analyzed by the NDP (Neutron Depth Profiling) method [9, 10] at the LVR-15 reactor [7], which made it possible to determine the depth distribution of lithium atoms (more precisely, the isotope  ${}^6\text{Li}$ , whose representation in the natural mixture of Li is  $\sim 7.5\%$ ) and its real changes depending on the charging of the sample. The NDP method (Fig. 2) uses a nuclear reaction with thermal neutrons  ${}^6\text{Li}(n_{\text{th}}, \alpha)\text{T}$  exhibiting a high cross Sect. (940 b) and a high reaction energy (4782 keV), where the reaction products (particles  $\alpha$  and T) are isotropically emitted with relatively high energies ( $\alpha$ : 2055 keV, T: 2727 keV), which can be easily distinguished from the unwanted exponential background (originating from the parasitic reactions of neutrons with the other structural elements of the composite and the substrate). The NDP method determines the instantaneous depth distribution of Li with a depth resolution nominally up to 10 nm, depending on the quality of the detector and the chosen experimental setup. When passing through the sample, alpha particles and tritons

lose part of their energy, so their residual energy determines, in principle, the original location of their parent lithium atoms in the sample. To obtain the Li depth distribution, an appropriate MC software, simulating the energy spectra, is needed. The NPI developer LIBOR [11] code and the commercially available SIMNRA [12] code were used in the experiment to evaluate the energy spectra. For the NDP experiments were employed  $50 \text{ mm}^2$  fully depleted detectors (FDD, Canberra) located in the multifunctional vacuum chamber of the NDP spectrometer (Fig. 2). The measurements were performed on a thermal neutron beam of a mirror neutron guide (SwissNeutronics) with a flux of  $7 \times 10^7 \text{ cm}^2\text{s}^{-1}$  and a Cd ratio of  $\gtrsim 10^4$ , which can be obtained at a reactor power of 10 MW.

## Results and discussion

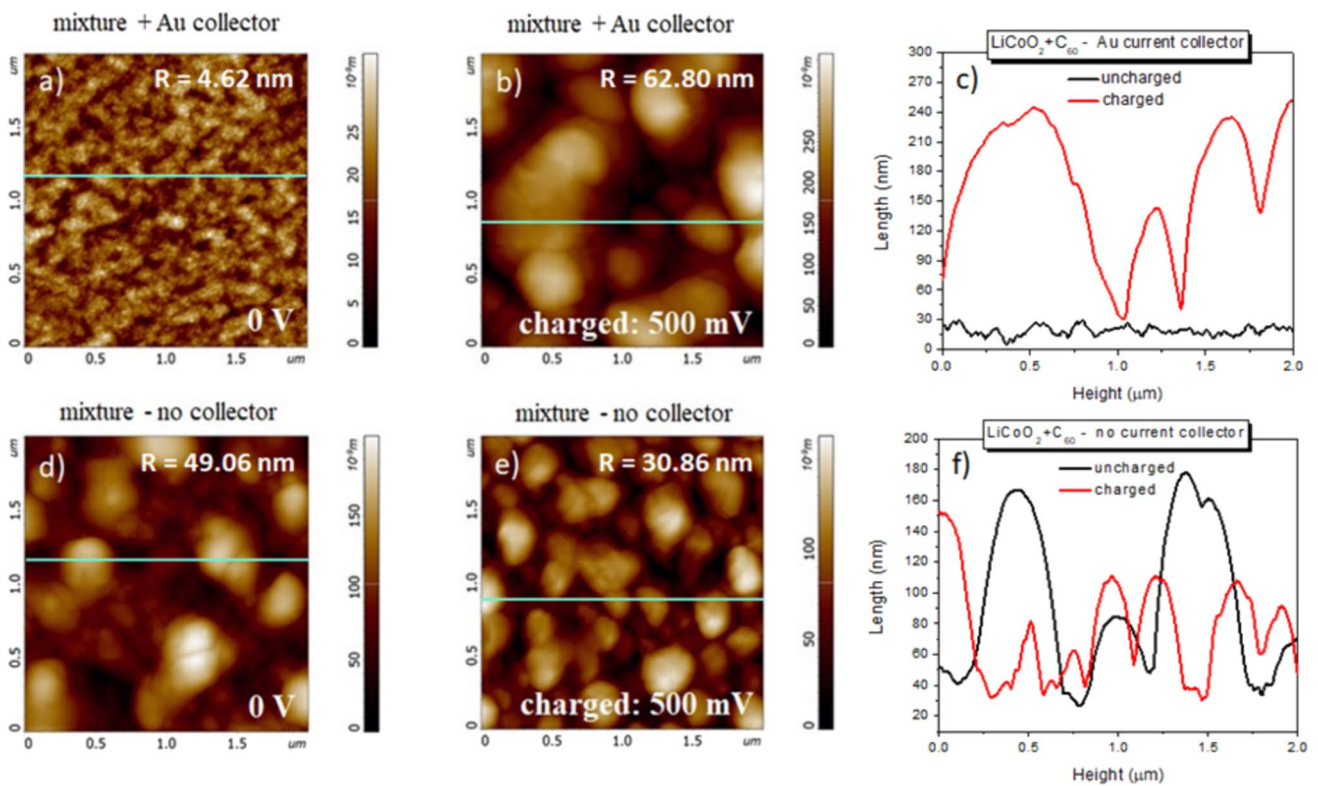
The following section presents the results of the study of thin layers of hybrid composites prepared as mixes or multilayers formed by  $\text{C}_{60}$  fullerenes and atoms (fragments) of the sputtered  $\text{LiCoO}_2$  target (with or without thin Au current collectors), where their two important aspects were monitored – the surface morphology of the samples and depth distribution of lithium (as charge carriers) depending on the applied voltage. As the study showed, both aspects are strongly influenced by each other.

Figure 3 shows the surface morphology of the samples of the mix (denoted as  $\text{LiCoO}_2 + \text{C}_{60}$ ) with and without Au collectors before and after charging at a voltage of 500 mV (AFM analyzes show that the changes in the surface morphology of



**Fig. 2** Sketch of the Neutron Depth Profiling (NDP) method of Li atoms consisting in measurement of the residual energies of the reaction products  $\alpha$  and T from the reaction of  ${}^6\text{Li}(n_{th}, \alpha)T$  with thermal

neutrons. The energy losses of the reaction products correspond to the thickness and type of sample material through which the reaction products pass



**Fig. 3** AFM micrographs of the surface morphology of the  $\text{LiCoO}_2 + \text{C}_{60}$  mixture with and without Au charge collectors before and after charging at a voltage of 500 mV: **a** mixture with Au collec-

tor before charging, **b** mixture with Au collector after charging, **c** line profiles for mixtures with Au collector before and after charging at 500 mV,

the composites are similar for all applied voltages, therefore only the data for the voltage of 500 mV, where the changes are most pronounced, are presented). AFM micrographs scanning a  $2 \mu\text{m} \times 2 \mu\text{m}$  area point to several interesting surface features of the hybrid microstructure formed:

- The surface of samples without Au collectors is composed of large particles with a lateral size of up to several hundreds of nm (d).
- After the deposition of Au, elongated structures with sizes of approx. 200 nm and widths  $< 100$  nm were formed on the surface of the mixtures, oriented to each other mostly in only a few directions (a). These formations in the form of grapes are composed of round nanoparticles with a size of 10–20 nm.
- After adding Au collectors, the surface roughness decreased significantly (about 10 $\times$ ), as indicated by micrographs a) and d) and confirmed by the line profile black curves in c) and f).
- The morphology of the mixes also changed dramatically after charging with an applied voltage of 500 mV – in the samples without Au collectors, the

roughness decreased by about 37% (see the change in line profiles (f)), but in the samples with Au collectors, the roughness increased sharply (approx. 13.5 $\times$ ), as demonstrated by the large change in the line profile (c).

**d** mixture without collector before charging, **e** mixture without collector after charging, **f** line profiles for mixtures without Au collector before and after charging at 500 mV.

Similar to the case of mixtures, an analysis of the development of the surface morphology of multilayers was carried out. Figure 4 shows in AFM micrographs ( $2 \mu\text{m} \times 2 \mu\text{m}$ ) how the surface morphology of the multilayers (labeled as  $\text{C}_{60}/\text{LiCoO}_2$ ) prepared with and without Au collectors changed before and after charging (this time at a voltage of 1000 mV). However, as can be seen, the morphology of the multilayers changed in a different way than it did for the mixtures:

- The surface of multilayers prepared without Au collectors is formed by large and relatively flat structures with sizes up to 500 nm (d).

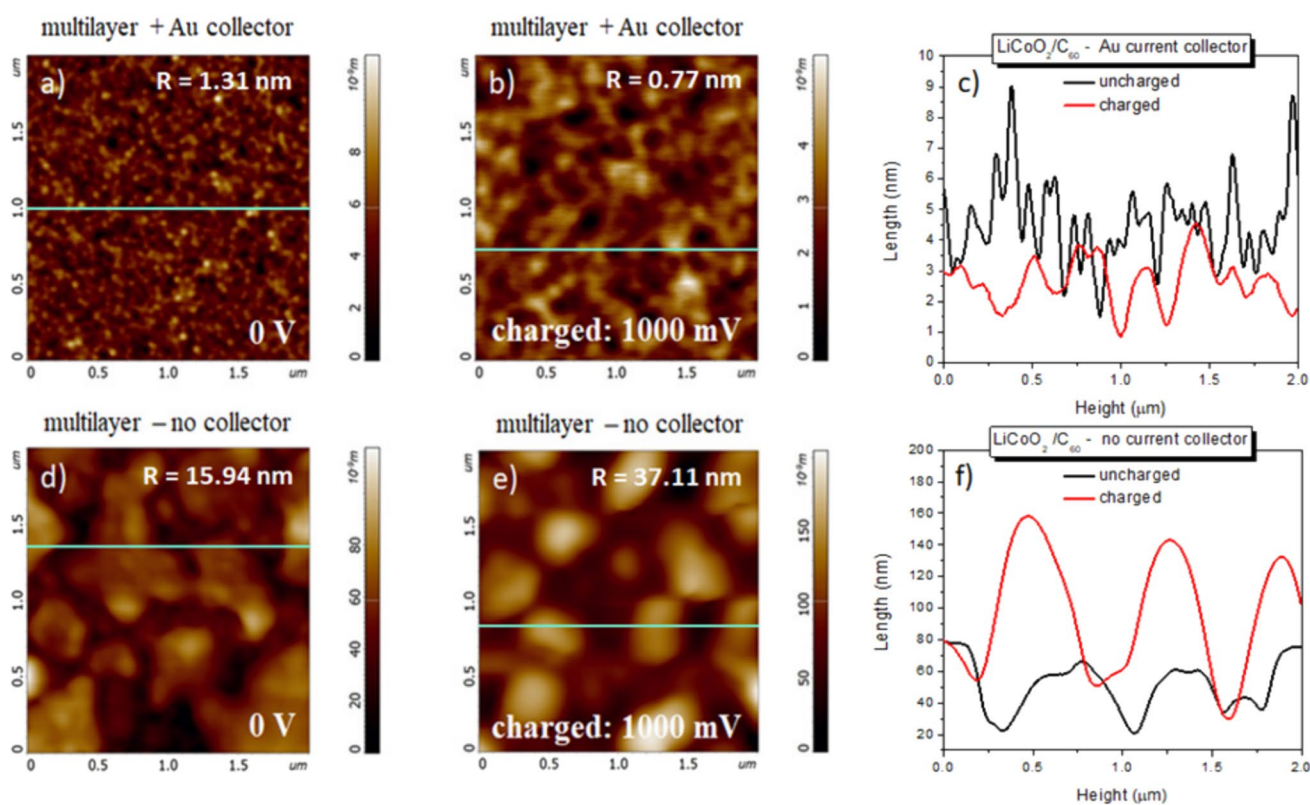


**Fig. 4** AFM micrographs of the surface morphology of the  $\text{C}_{60}/\text{LiCoO}_2$  multilayer with and without Au charge collectors before charging and after charging at a voltage of 1000 mV: **a** multilayer with Au collector before charging, **b** multilayer with Au collector after charging, **c** line profiles for the multilayer with Au collector

before and after charging at 1000 mV, **d** multilayer without collector before charging, **e** multilayer without collector after charging, **f** line profiles for multilayer without Au collector before and after charging at 1000 mV

- (ii) In the case of multilayers with Au collectores, the structure of separate flat domains disappeared and a morphology consisting of densely packed grains with sizes of only a few nm emerged (a).
- (iii) After the addition of Au collectors, the surface roughness of multilayers also decreased significantly (approx. 12x), see micrographs a) and d) and black curves in line profiles c) and f).
- (iv) Dramatically (but opposite to the mixture!) the morphology changed after charging at a voltage of 1000 mV – without Au collectors the surface roughness is approx. 2.3 x greater (see line profiles (f)), however, in multilayers with Au collectors the roughness decreased approx. by 40%, as demonstrated by a significant change in the line profile (c).

In general, it can be concluded that the development of the surface morphology of the hybrid composites ( $\text{LiCoO}_2 + \text{C}_{60}$  a  $\text{C}_{60}/\text{LiCoO}_2$ ) will be related to the change of their microstructure depending on the charging process (i.e., the applied voltage). The more pronounced the change in the depth profiling of building elements, the greater will be the change in the roughness of their surface, for example. Closely related to this is the electrochemical activity of building elements given by their electrochemical potential [Li (−3.04 V), Co (−0.292 V), O (+1.25 V), C (+0.207 V), Au (+1.83 V)]. In composites where the building elements are randomly distributed (e.g., in a mixture), it can be expected that the microstructure created will show local stress and, as a result, also a higher surface roughness. In contrast, composites

formed by layers of chemical compounds (e.g., multilayers) will be more stable, and therefore with a lower surface roughness. If both types of composites are supplemented with thin charge collectors, it can be expected that the roughness on their surface will be significantly reduced and will be higher only where the surface roughness of the layer under the collector was high. In the case of connecting an external voltage and carrying out the charging process, it can also be expected that electrochemically active elements (especially Li ions) penetrate through the collector to its surface and form there randomly Li clusters [3, 13]. In this case, the surface roughness of the sample will also increase sharply. In multilayers with an electrochemically less active fullerene layer, acting as a barrier between the collector and the  $\text{LiCoO}_2$  buffer layer, Li ions will penetrate through the fullerene layer into the charge collector to a lesser extent than with the previous type of composite, so the surface roughness can be expected to be lower. As can be seen, the surface morphology of complex composites really depends on their microstructure, which can be affected by external influences, e.g., applied voltage, acting strongly on their electrochemically active structural elements (Li in particular). In order to confirm these general assumptions, which agree with the results of the presented AFM analyses, measurements of lithium depth profiles in both hybrid composites were performed for all applied voltages. The results are given in the following paragraphs.

Figure 5 shows the results of measuring the energy spectra (more precisely, only the alpha part) from the  ${}^6\text{Li}(n,\alpha)\text{T}$  reaction that takes place in a thin  $\text{LiCoO}_2 + \text{C}_{60}$  mixture

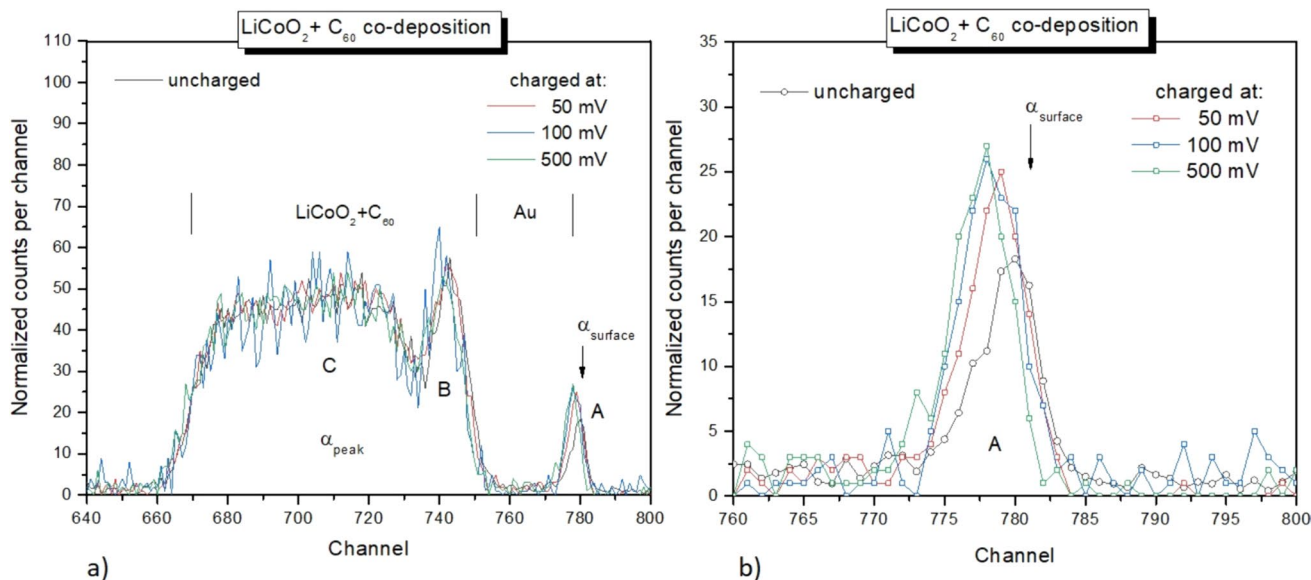


**Fig. 5** NDP spectra (alpha parts only) from the reaction of  ${}^6\text{Li}(n,\alpha)\text{T}$  of thermal neutrons with lithium atoms in  $\text{LiCoO}_2 + \text{C}_{60}$  composite with gold charge collectors before and after charging at voltages of

50, 100 and 500 mV. The spectra consist of several peaks marked as A, B and C (a), where peak A (b) corresponds to the presence of Li in the Au collector, respectively on its surface

with Au collectors (NDP study of mixtures without Au collectors are not presented here, their spectra did not show any significant changes during charging). Energy spectra were measured before and after charging the composite at voltages of 50, 100 and 500 mV. The given spectra (normalized to the same neutron flux fluence) correspond to alpha particles emitted in  ${}^6\text{Li}(n,\alpha)\text{T}$  reactions from the subsurface layers (a), respectively from the surface layer of the composites formed by the Au electrode (b) (spectra of tritons are irrelevant for the study and are therefore also not presented here). As can be seen, lithium (and it can be assumed that the other building elements as well) are unevenly distributed in the composite (zones with higher and lower concentration are recorded). Moreover, as a result of charging, the depth

profiles (i.e., relative concentration vs. depth) of lithium (and probably also of other structural elements) changes. This can be seen, for example, at the surface peak A, where the relative concentration of Li increases with the applied voltage.

Figure 6 shows the results of the simulation of the measured NDP spectra (i.e., the depth distributions of Li and other building elements sandwiched between the Au charge collectors) before and after charging at voltages of 50, 100 and 500 mV. The simulation of energy spectra was performed using the LIBOR and SIMNRA codes. As can also be seen, lithium is distributed in 3 broad areas (A, B and C) in the composite, while other structural elements are located only in areas B and C (Au only in part A).

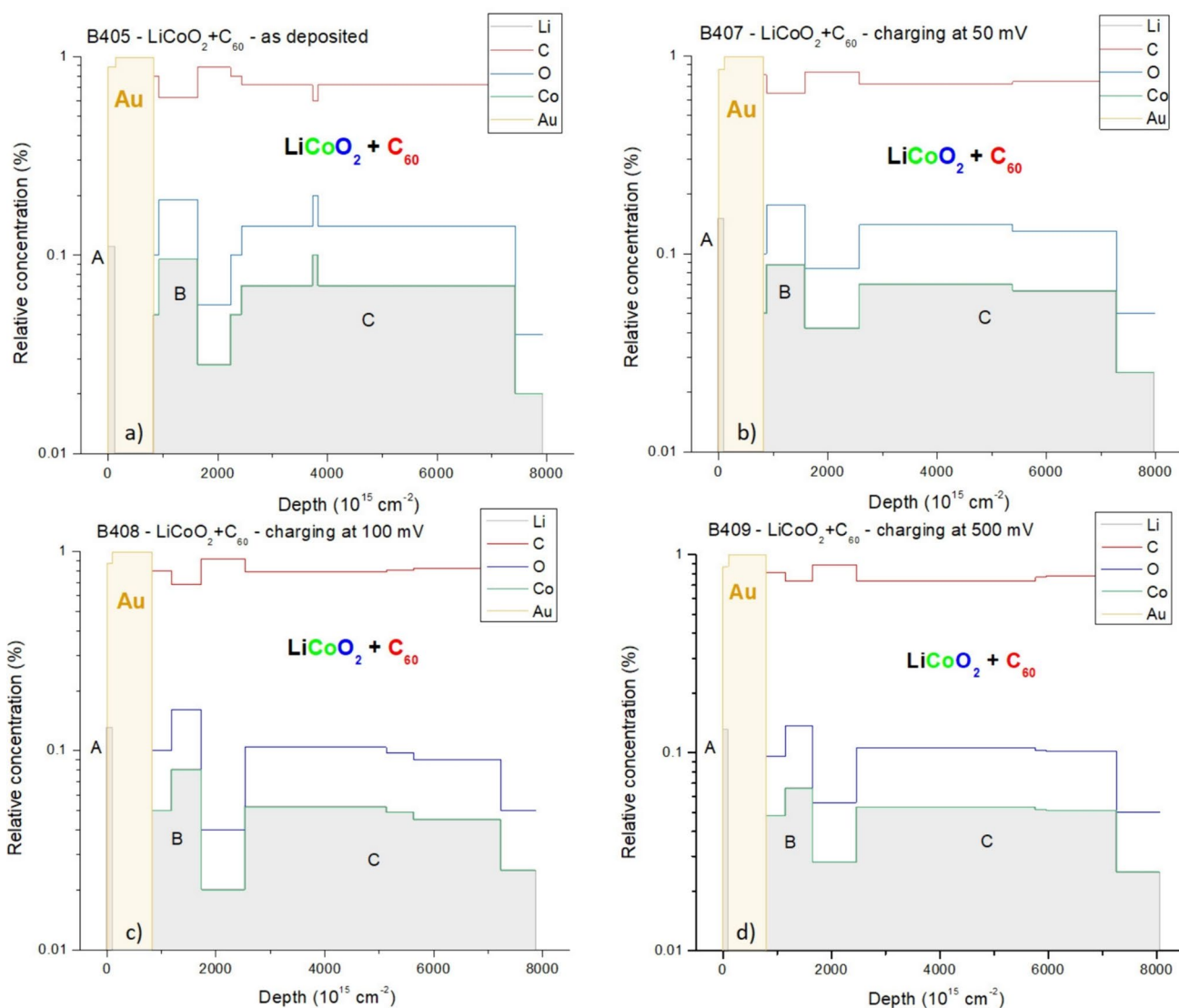


**Fig. 6** Simulation results of NDP spectra from the reaction of  ${}^6\text{Li}(n,\alpha)\text{T}$  of thermal neutrons with Li in the  $\text{LiCoO}_2 + \text{C}_{60}$  mixture, supplemented with Au charge collectors, depending on the applied

voltage: as deposited (a), 50 mV (b), 100 mV (c) and 500 mV (d). The simulation of the element depth profiles was performed using the LIBOR and SIMNRA codes

The relative concentration of elements in individual parts changes depending on the charging process.

The MC simulations show that as a result of the applied voltage there is a transport (diffusion) of unbound (or weakly bound) lithium ions between regions A, B and C, and simulations of the spectra indirectly indicate also a possible redistribution of other elements (in order to create a suitable fit, which would correspond as best as possible to the measured spectrum, while maintaining the stoichiometric ratio of the building elements of the  $\text{LiCoO}_2$  compound, it was necessary to change correspondingly the relative concentration of the other elements Co, O and C with depth).

An interesting aspect that dominates the measured NDP spectra is the large dip in the spectra between region B and C. The dip is about a third of the area of a peak B for the pre-charged sample and half for the charged samples, indicating a significant cause that led to such a drop in Li concentration. To shed some light, the NDP spectra of  $\text{LiCoO}_2 + \text{C}_{60}$  without a charge collector were measured to verify the effect of the Au collector on the distribution of Li in the composite. The resulting spectrum (not given here) showed a broad and continuous alpha peak that had none of the dip seen in the mixture samples with Au collectors.

The result thus indicates that the electrochemical potentials of the two elements Li ( $-3.04$  V) and Au ( $+1.83$  V) play an important role in the distribution of Li in the mixtures [14, 15]. These cause that, even without an external voltage, Li diffuses from the inside towards the Au collector (and eventually to the surface), while a larger part of Li accumulates in front of the collector from the inside. The NDP data show a broad zone of increased Li concentration (region B) and an associated decrease in Li concentration

in the adjacent zone below (i.e., dip between the peaks B and C).

Figure 7a shows the course of the ratio of the peak areas  $A/(B+C)$  and  $B/C$  on the voltage applied during charging of the composite. As can be seen, depending on the voltage level, the Li concentration redistributes in the indicated zones not only between the surface (peak A) and the subsurface environment (bi-peak  $B+C$ ), but also between both subsurface peaks B and C. The apparent cause of these changes is the diffusion of Li ions induced by the applied voltage. As can also be seen from Fig. 7a, the total amount of Li that has spontaneously diffused into the Au collector and onto its surface is about 3.5% of the total number of Li atoms in the sample bulk. The reason for such behavior can be attributed, as indicated above, to the different electrochemical potentials of the structural elements, which can act on Li atoms as a driving force for their migration [14, 15]. Figure 7a also indicates that with the applied voltage, there is a gradual increase in the amount of Li atoms in the peak A up to the level of approx. 4.5% (at 100 mV), when the ratio becomes evidently saturated (a higher applied voltage already leads to a decrease in the Li concentration). In addition, Fig. 7a also quantifies the ratio of Li contents in B and C as a function of the applied voltage, showing that as the voltage increases, Li atoms move from C to B, so the amount of Li in B increases, and at a voltage of 500 mV, the ratio of  $B/C$  is higher by almost 15% compared to the sample before charging. At the same time, however, it is necessary to mention that during charging there is an outflow of Li ions from B to A (however, this amount is about an order of magnitude smaller than the transfer of Li between B and C). Figure 7b shows in detail how the number of Li

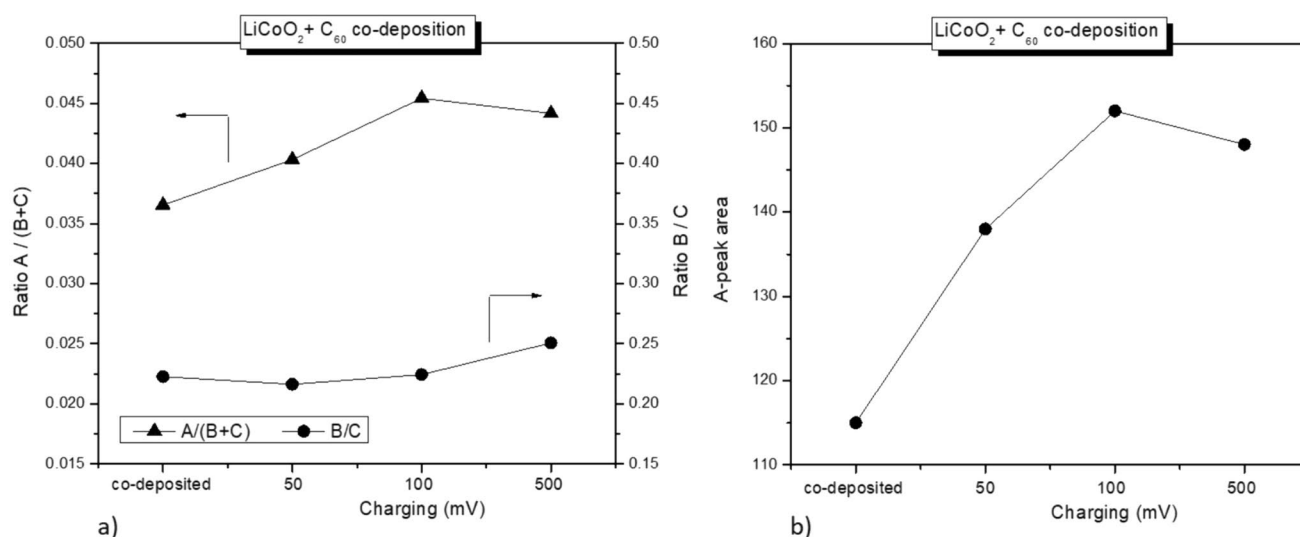


**Fig. 7** **a** Evolution of the area ratios  $A/(B+C)$  and  $B/C$ , i.e., surface peak A to the subsurface bi-peak ( $B+C$ ), and ratio of two subsurface peaks  $B/C$ , before and after charging at 50, 100 and 500 mV; **b** growth of the surface peak A initiated by charging of  $\text{LiCoO}_2 + \text{C}_{60}$

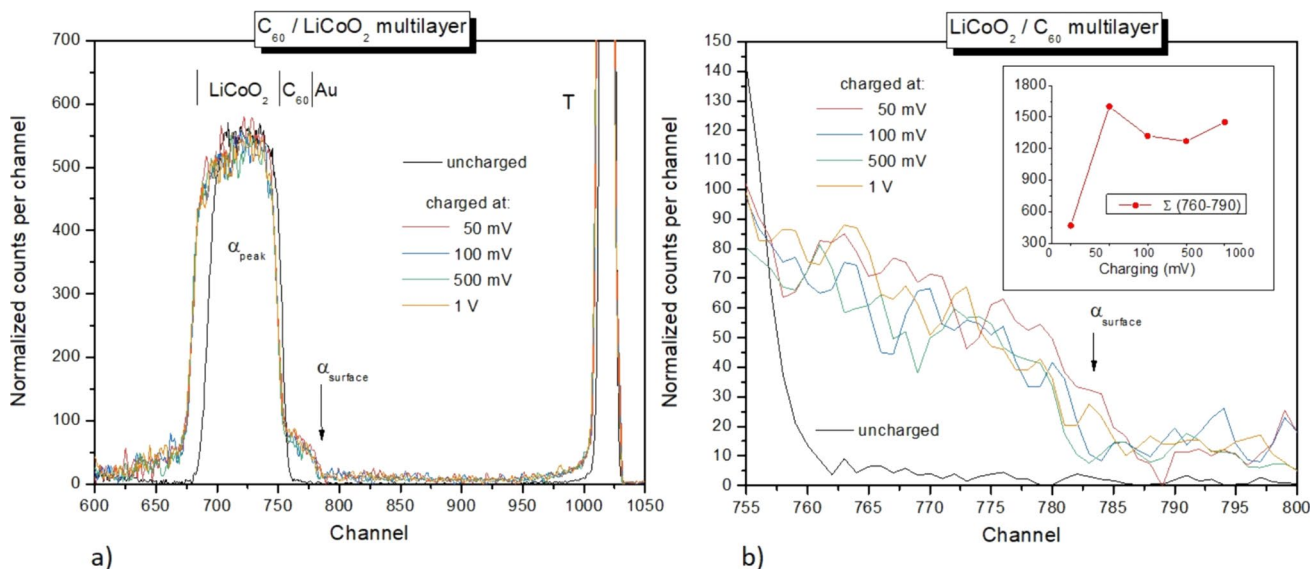


ions increases with the applied voltage in the area of the Au collector (and on its surface). However, for higher voltages, the proportion of increase gradually decreases, so it can be assumed that for voltages  $> 500$  mV the increase in Li concentration will saturate to a level that is about 20% higher than the Li concentration of the composite before charging.

In Fig. 8 are energy spectra from the  ${}^6\text{Li}(n,\alpha)\text{T}$  reaction showing both alpha and triton parts, measured for multilayers (labelled  $\text{C}_{60}/\text{LiCoO}_2$ ) with an Au charge collector. NDP analysis was performed before and after charging the composite at voltages of 50, 100, 500 and 1000 mV. The measured spectra are normalized to the same neutron flux fluence, the spectrum measured before charging corresponds to a sample that was prepared with a thinner layer of  $\text{LiCoO}_2$ , which manifests itself as a narrower alpha peak and also triton peak. In this sample, a thinner layer of the upper gold collector was also deposited, which led to a slight shift of the alpha peak to higher energies (see Fig. 8a, black spectrum); for the triton peak the advance is not seen due to the lower energy resolution of tritons compared to alpha. As can be seen, within the statistical error, the alpha spectra for the charged composites are very similar, with the fact that, unlike the spectrum measured before charging, they all show a new broad satellite peak in the region between channels 760 and 790 (i.e., in the Au collector and the upper part of the fullerene layer beneath). The alpha particles observed in this region are emitted from Li ions that, due to charging, have drifted towards the gold collector and onto its surface. A more detailed analysis shows (Fig. 8b) that the Li increase

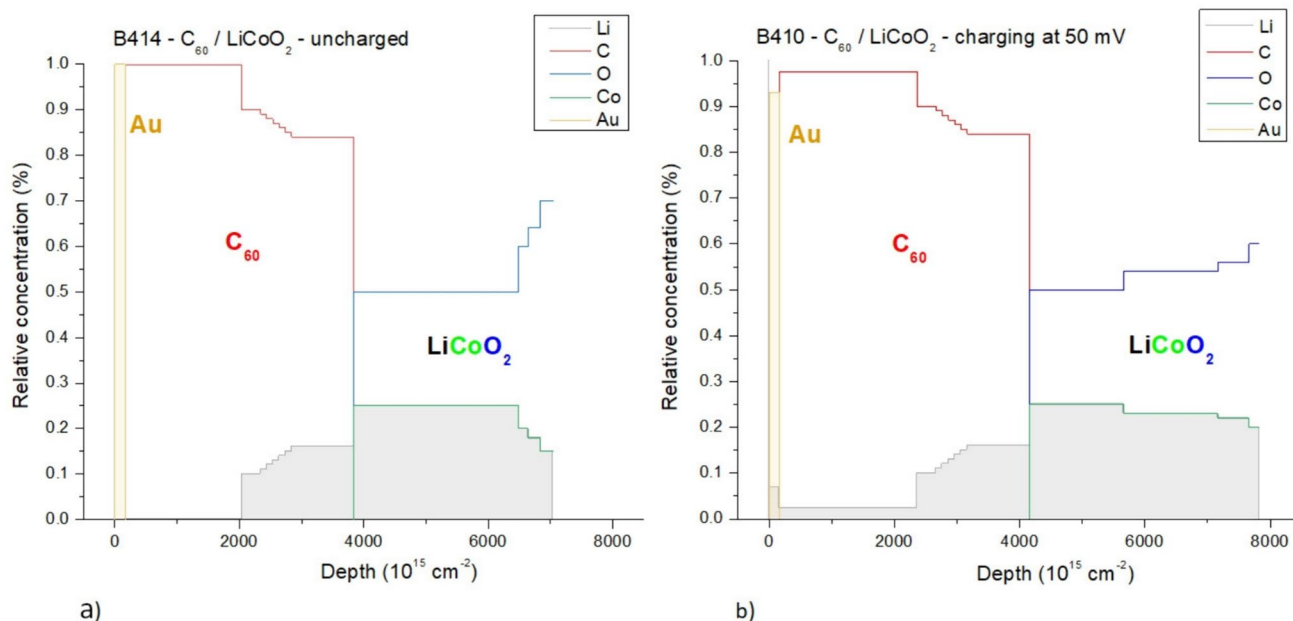
in the satellite peak is sharp, especially when charging at 50 mV. Charging at higher voltages is no longer as effective, although it leads to an increase in concentration, but by approx. 10–20% lower, which indicates saturation of the amount of Li in the collector area, or redistribution of Li back towards the composite. After evaluating the depth profiles, it became clear that during charging only about 3–4% of Li ions were transported to the area of the Au collector and the upper part of the fullerene layer from the total amount of Li contained in the composite. However, this is an amount that is comparable to the total volume of Li ions that was deposited into the Au collector and onto the surface of the  $\text{LiCoO}_2 + \text{C}_{60}$  mix (see Fig. 7a).

Figure 9 shows the simulation results of the NDP spectra measured for a  $\text{C}_{60}/\text{LiCoO}_2$  multilayer with Au collectors before charging (a) and after charging at 50 mV (b) (depth profiles for multilayers charged at voltages of 100, 500 and 1000 mV showed no changes compared to the profile (b) and are therefore not presented here). When comparing the two profiles shown, their difference is clearly visible, especially for lithium, where the uncharged multilayer completely lacks the signal from Li in the surface region ( $0\text{--}2000 \times 10^{15} \text{ Li cm}^{-2}$ ), including the Au collector and the upper part of the fullerene layer, while multilayers charged at a voltage of 50 mV, the presence of Li is recorded in the entire indicated area, including the surface itself. The depth profiles further show that in the deeper part of the fullerene layer there is a significant amount of Li (up to 15%), which penetrated there from the buffer layer of previously deposited  $\text{LiCoO}_2$ . In the



**Fig. 8** a NDP spectra (both alpha and triton parts) from the reaction of  ${}^6\text{Li}(n,\alpha)\text{T}$  of thermal neutrons with lithium atoms in a  $\text{C}_{60}/\text{LiCoO}_2$  multilayer with Au charge collectors before charging and after charging at voltages of 50, 100, 500 and 1000 mV; b the upper edge of the alpha spectrum with a satellite peak in the region of channels 760–

790 showing the increase of Li ions into the gold charge collector of the sample at the applied voltage; inset shows the dependence of the satellite peak area on the applied voltage confirming its initial sharp rise and subsequent variable saturation



**Fig. 9** Simulation results of NDP spectra from the reaction of  ${}^6\text{Li}(n,\alpha)\text{T}$  of thermal neutrons with Li in the  $\text{C}_{60}/\text{LiCoO}_2$  multilayer with Au charge collectors depending on the applied voltage:

deep areas of the composite, there is seen a slight decrease in Li, which could be due to the diffusion of the active Li atoms into the buffer Au collector and the Si substrate, as also recorded in other studies [16, 17].

## Conclusions

As it turned out, by the deposition of building elements Li, Co, O and C, carried out by a combination of ion sputtering of the  $\text{LiCoO}_2$  target and simultaneous evaporation of fullerenes, thin layers of  $\text{LiCoO}_2 + \text{C}_{60}$  mixtures can be prepared. The composites consist of hybrid nanoparticles (based on  $\text{LiCoO}_2$  and  $\text{C}_{60}$ ) and free (or weakly bound) Li atoms that exhibit strong electrochemical activity. Due to the significant difference between the chemical potentials of Li and other elements, a spatial redistribution of Li atoms occurs: (i) the spontaneous formation of a large enriched / depleted bi-zone beneath the Au collector, and (ii) considerable diffusion of Li through the Au collector on its surface. When applying a small electric bias ( $< 1$  V), an additional driving force is created, which deepens the division of the subsurface bi-layer and increases the diffusion and penetration rate of Li ions into the Au collector and onto its surface. It was estimated that about 4.5% of the Li atoms deposited in the composite will participate in this process. As a result of these changes, there is also a sharp increase in the roughness of the surface morphology.

as deposited (a), 50 mV (b) (depth profiles at other voltages did not change, so they are not listed). The simulation of depth profiles was performed using the LIBOR and SIMNRA codes

Similarly, thin  $\text{C}_{60}/\text{LiCoO}_2$  multilayers can also be prepared by ion sputtering of the  $\text{LiCoO}_2$  target with subsequent evaporation of fullerenes, which also contain free (or weakly bound) Li atoms. It turns out that in a multilayer with a fullerene layer, spontaneous diffusion of Li into the Au collector does not occur, but when a small bias voltage ( $< 1$  V) is applied, Li ions penetrate the fullerene layer and diffuse into the collector and onto its surface in a relatively large amount (about 4% of the total number of the deposited Li atoms). It is a similar amount to the  $\text{LiCoO}_2 + \text{C}_{60}$  mixture. Due to the more even arrangement of the elements in the multilayer system and the milder penetration of Li ions on the surface of the composite, the surface morphology did not change much and the surface roughness remained at a low level.

In conclusion, it can be stated that the attempt to create thin hybrid composites that would exhibit electrochemical activity suitable for an energy storage system was successful in that the possibility of their production was verified using the method of ion sputtering of a  $\text{LiCoO}_2$  target in combination with the evaporation of fullerenes, and their electrochemical reactions to applied external tension. In further research, however, it is necessary to specify the performed experimental steps – for example, it is necessary to determine the proportion of free (or weakly bound) Li atoms in the composites and to find their optimal microstructure to maximize it.

**Acknowledgements** This work was supported by the Ministry of Education, Youth and Sports (MEYS) CR under the project OP JAK CZ.02.01.01/00/22\_008/0004591. The authors acknowledged also the support of Czech Academy of Science Mobility Plus Project, Grant No. JSPS-24-12. Measurements were carried out at the CANAM infrastructure of the NPI CAS Rez under project LM 2015056. The employment of the CICRR infrastructure supported by MEYS project LM2023041 is acknowledged.

**Funding** Open access publishing supported by the National Technical Library in Prague.

**Open Access** This article is licensed under a Creative Commons Attribution 4.0 International License, which permits use, sharing, adaptation, distribution and reproduction in any medium or format, as long as you give appropriate credit to the original author(s) and the source, provide a link to the Creative Commons licence, and indicate if changes were made. The images or other third party material in this article are included in the article's Creative Commons licence, unless indicated otherwise in a credit line to the material. If material is not included in the article's Creative Commons licence and your intended use is not permitted by statutory regulation or exceeds the permitted use, you will need to obtain permission directly from the copyright holder. To view a copy of this licence, visit <http://creativecommons.org/licenses/by/4.0/>.

## References

- Hao J, Li X, Song X, Guo Z (2019) Recent progress and perspectives on dual-ion batteries. *EnergyChem* 1(1):100004
- Zhang C (2019) High-voltage electrolytes. *Nat Energy* 4(5):350
- Cannav'ò A, Tomandl I, Lavrentiev V, Lavrentieva I, Ceccio G, Kormunda M, Jagerova A, Kobayashi T, Sassa T, Vacik J (2022) Delithiation dynamics of the LICGC electrolyte out of the voltage limits. *Surf Interfaces* 33:102207
- Fan T, Wang Y, Harika VK, Nimkar A, Wang K, Liu X, Wang M, Xu L, Elias Y, Sclar H, Chae MS, Min Y, Lu Y, Shpigel N, Aurbach D (2022) Highly stable 4.6 V LiCoO<sub>2</sub> cathodes for rechargeable Li batteries by rubidium-based surface modifications. *Adv Sci* 9(33):2202627
- [cas.cz/canam](http://cas.cz/canam)
- [www.cicrr.cz](http://www.cicrr.cz)
- [www.cvrez.cz](http://www.cvrez.cz)
- Schönherr E, Matsumoto K, Freiberg M (1999) On the evaporation of C<sub>60</sub> in vacuum and Inert gases at temperatures between 830 K and 1050 K. *Fuller Sci Technol* 7:455–466
- Downing RG, Lamaze GP, Langland JK, Hwang ST (1993) Neutron depth profiling: overview and description of NIST Facilities. *J Res Natl Inst Stand Technol* 98:109–126
- Vacik J, Tomandl I, Hnatowicz V, Horak P, Cannavo A, Ceccio G, Fink D, Kobayashi T, Rongbin Y, Baba M (2019) Study of Li diffusion in thin Li-ion batteries by thermal neutron depth profiling (TNDP). *AIP Conf Proc* 2160:03005
- Hnatowicz V, Vacik J, Fink D (2010) Deconvolution of charged particle spectra from neutron depth profiling using simplex method. *Rev Sci Instrum* 81:073906
- [mam.home.ipp.mpg.de/index.html](http://mam.home.ipp.mpg.de/index.html)
- Tomandl I, Kobayashi T, Cannavo A, Vacik J, Ceccio G, Sassa T, Hnatowicz V (2022) Investigation of lithiation/delithiation processes in ceramic solid electrolyte by means of Neutron depth profiling. *J Power Sources* 542:231719
- Ko S, Obukata T, Shimada T, Takenaka N, Nakayama M, Yamada A, Yamada Y (2022) Electrode potential influences the reversibility of lithium-metal anodes. *Nat Energy* 7:1217–1224
- Gao J, Shi S-Q, Li H (2016) Brief overview of electrochemical potential in lithium ion batteries. *Chin Phys B* 25:018210
- Wang H, Ji X, Chen C, Xu K, Miao L (2013) Lithium diffusion in silicon and induced structure disorder: a molecular dynamics study. *AIP Adv* 3:112102
- Seidlhofer BK, Jerliu B, Trapp M, Huger E, Risse S, Cubitt R, Schmidt H, Steitz R, Ballauff M (2016) Lithiation of crystalline silicon as analyzed by operando neutron reflectivity. *ACS Nano* 10:7458–7466

**Publisher's note** Springer Nature remains neutral with regard to jurisdictional claims in published maps and institutional affiliations.